Iraqi Journal of Science
ISSN: 0067-2904
GIF: 0.851

Efficient Method for Color Iris Localization

Esraa G. Daway[1*], Loay E.George[2], Radhi Sh.Hamoudi[1]
[1]Department of Physics, College of Education, Almustanserya University, Baghdad, Iraq
[2]Department of Computer Science, College of Science, University of Baghdad, Baghdad, Iraq

Abstract
Iris detection is considered as challenging image processing task. In this study efficient method was suggested to detect iris and recognition it. This method depending on seed filling algorithm and circular area detection, where the color image converted to gray image, and then the gray image is converted to binary image. The seed filling is applied of the binary image and the position of detected object binary region (ROI) is localized in term of it is center coordinates are radii (i.e., the inner and out radius). To find the localization efficiency of suggested method has been used the coefficient of variation (CV) for radius iris for evaluation. The test results indicated that is suggested method is good for the iris detection.

Keywords: iris, localization, Isolation, recognition.

الطريقة الفعاليه لتحديد القزحيه الملونه

اسراء كاطع دواي[1]*، لؤي ادور جورج[2]، راضي شدهان الطويل[1]
[1]قسم الفيزياء ، كلية التربيه ، الجامعه المستنصريه، بغداد، العراق
[2]قسم الحاسبات، كلية العلوم، جامعة بغداد، بغداد، العراق

الخلاصه
ان تميز القزحيه له دور مهم في كثير من تطبيقات المعالجه الصوريه ،في هذه الدراسه تم اقتراح خوارزميه جديده تعتمد على طريقة حشو البذره وكشف الدائره ،حيث يتم تحويل الصوره الملونه الى صور ذات تدرجات رماديه ومن ثم يتم تحويلها الى ثنائيه وطبقت عليها حشو البذره تم تحديد مواقع كشف الدائري في الصوره الثنائيه والتي اسقطت على الصوره الاصليه . من اجل استخراج القزحيه فقط لمعرفة كفاءة هذه الطريقه المقترحه تم اعتماد مقياس معامل التباين لنصف القطر ومن خلاله تبين ان الطريقه المقترحه هي طريقه جيده.

1. Introduction

With the increasing emphasis on security, automated personal identification based on biometrics has been receiving extensive attention over the past decade. Biometrics aims to accurately identify each individual using different physiological or behavioral characteristics, such as fingerprints, iris, face, retina, gait, palm-prints and hand geometry (Jain et al., 1999; Zhang,2000). Recently, iris recognition is becoming an active topic in biometrics due to its high reliability for personal identification [1] (Jain et al., 1999; Mansfield et al. 2001; Daugman, 2003). Iris localization is a key step in iris recognition; it isolates the iris part in eye image by detecting both the inner and outer boundaries of iris area. The overall performance of an iris recognition system is highly related to the localization accuracy [2]. The accurate pupil detection, as the inner iris boundary, is the most important and the first step in iris localization (Kheirolahy et al., 2009). Numerous methods were proposed to locate the pupil; they based on the fact that the pupil edge can be estimated as circular shape**.**

*Email: esraado2007@yahoo.com

2. The Iris

Human eye iris is a visible color ring bounded by the pupil (the dark opening) and white sclera, as depicted in Figure-1.

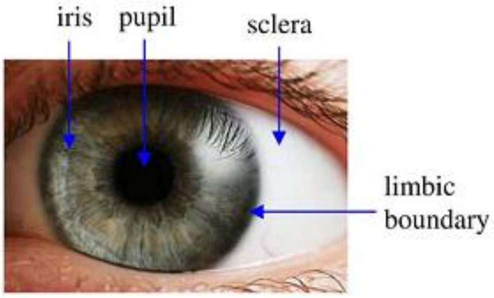

Figure 1- Anterior surface of the iris

The iris is suspended in aqueous humor, behind the cornea but in front of the lens as shown in Figure2.

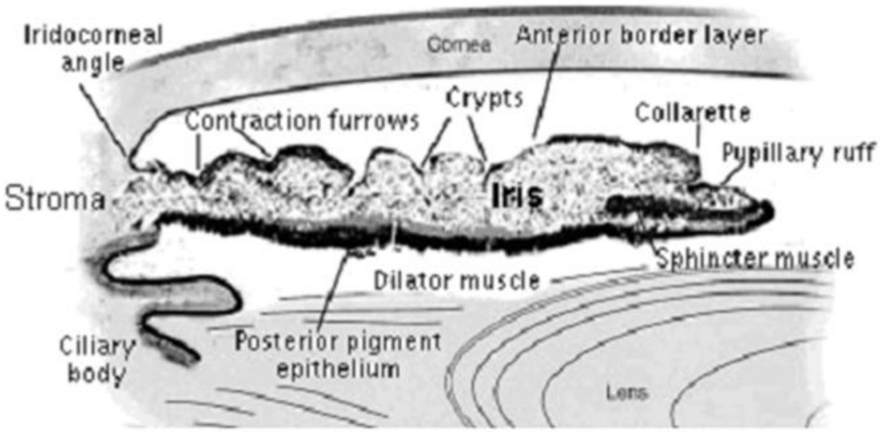

Figure 2- Anterior segment of the eye (Modified from [3]).

The iris divides the space between the lens and the cornea into the anterior chamber (between the cornea and the iris) and posterior chambers (between the iris and the lens). The periphery of the iris is attached to its root at the iridocorneal angle of the anterior chamber where it merges with the tissue inside the eye: the ciliary body and trabecular meshwork. The free edge of the iris is known as the pupillary margin or pupillary ruff (the boundary of the pupil). The formation of the human iris begins during the third month of gestation; its distinguishable pattern is completed by the eight month of gestation, but pigmentation continues into the first year after birth [4]. The size of the iris varies from person to person with a range of 10.2 to 13.0 mm in diameter [5], an average size of 12 mm in diameter, and a circumference of 37 mm [6,7].

3. The Proposed Iris Localization System

In this work an iris localization system is developed and implemented. It consists of three main stages, as shown in Figure-3.

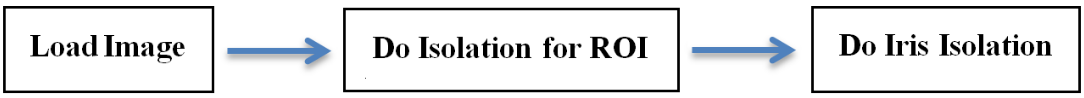

Figure 3-The main stages of the Iris Localization system

In the following the steps of theses main stages are given:

3.1 Load Image Data

As first stage the color image data is located from the image data as raster file consist of 3 colors component (Red, Green, Blue), and then finding the lightness according to the following equation (1), as shown in Figure-4.

$$g\,(x,y) = \frac{1}{3}\big(Red(x,y) + Green(x,y) + Blue(x,y)\big) \quad (1)$$

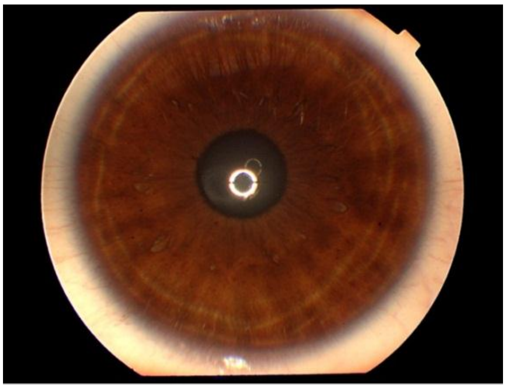

Figure 4- An example of fundus area

3.2 Isolation for ROI (Region of interest)

In put: color image with band R (wid,hgt), G (wid,hgt), B(wid,hgt)
Output: rad //Rad in for ROI
This step includes sub steps as following:
A. Calculate the Histogram for the gray image using the equation:

$$\boldsymbol{Hist(i) = \frac{N(i)}{N}} \quad (2)$$

Where, $N = Width_{Image} \times Height_{Image}$ is the size of image. N_i is the frequency of occurrence of gray level (i).
B. Binarization by Thresholding: if implies the following
(i) Finding Threshold value G
G = 0
While His(G) > His(G + 1) And His(G) > 100
    G = G + 1
End while
(ii) Make binarization by thresholding. The central part holds the darkest pixels (which are flagged 1, while other pixels are flagged 0).
Set the array dimension: Bin(Wm, Hm)
For Y = 0 To Hm: For X = 0 To Wm
    If Gry(X, Y) <=Threshold Then Bin(X, Y)=0 Else Bin(X, Y)=1
Next X: Next Y
C. Remove the small isolated areas (i.e., islands/gaps) using seed filling algorithm.
D. Calculate the Center Point Coordinates and Radius of the Bright Area, using the following equation:

$$\boldsymbol{x_{cen} = \frac{1}{n}\sum_{i=1}^{n} x_i\ , \quad s_y = \frac{1}{n}\sum_{i=1}^{n} y_i\ , \quad R = \sqrt{\frac{n}{\pi}}} \quad (3)$$

Where, n is the number of collected white pixels; (x_i, y_i) are the coordinates of the i^th collected bright pixel.
E. Establish the Mask of the Brightest Area, Bin(), that represents the Isolated ROI region area, as shown in Figure-5. The following shown steps are for establishing the mask:
For all y value
  $dy = y - y_c$
  If $dy \le R$ then
    For all x value
      $dx = x - x_c$
      if $(dx)^2 + (dy)^2 < R$ then Bin(x, y)=1 else Bin(x,y)=0
    Next
Figure-6 shows a sample of the established mask:

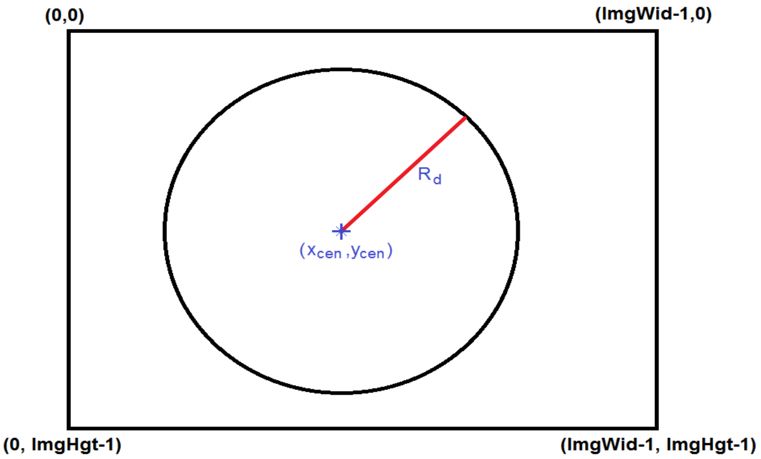

Figure 5- The isolation of ROI as circle region

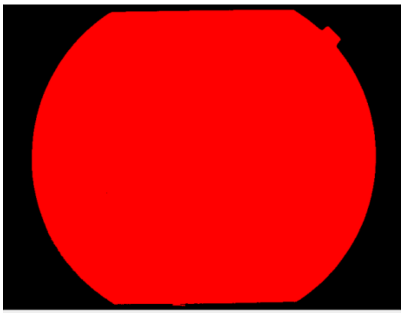

Figure 6- The Mask Image output of do Isolation for ROI (Region of interest)

3.3 Iris Isolation

In put: G (wid,hgt), B(wid,hgt) with size x,y

Output: Iris Isolation.

In this stage the iris is isolated from the ROI region by using following steps:

A. Calculate the Mean (*m*) & Standard Deviation (σ) [8] of the Pixels belong to ROI by applying equations (4) and (5).

For all x and y values DO

If Bin (x,y)=1

$$m = \frac{1}{N}\sum \boldsymbol{G(x,y)} \quad (4)$$

$$\boldsymbol{\sigma} = \sqrt{\sum_{x,y} \boldsymbol{G^2(x,y) - m^2}} \quad (5)$$

B. Apply Linear Contrast Stretching and calculate the mean of the established stretched image, the applied Contrast Stretching for gray image was performed only on the pixels belong to ROI .The stretching step is applied using the following equation (6):

$$Ics = \begin{cases} 0 & if\ G \leq Min \\ 255\dfrac{(G-Min)}{Max-Min} & if\ Min < G < Max \\ 255 & if\ G \geq Max \end{cases} \quad (7)$$

Where, *Min*=*m*–σ and *Max*=*m*+σ.

C. Do Binarization by Thresholding: The gray image is converted to binary image using the mean value as threshold value.

```
For all x value
   For all y value
      If Bin(X, Y) = 1 Then
         If tImg(X, Y) >= Mean Then tImg(X, Y) = 1 Else tImg(X, Y) = 0
      End if
   Next y
Next x
```

D. Do Tiling; Repeatedly, to remove the white points appeared in the binary image, after converting the image to binary, the image conform two regions as same circle (white and background black). The edge region includes some noise points, to remove this point we used tiling:
tImg(X, Y)=Tiling(I_{cs} (X,Y))
E. Apply seed filling to remove gaps and islands in the iris region [9].
F. Remove the boundary points using a window (with size 3x3):
Set Bin(X,Y)=1 iff (x,y) is a location not close to boundary of the region
Otherwise set Bin(X,Y)=0
G. By using the modified mask, Bin(), re-establish the binary image from the gray image.
H. Invert the Binary Representation of the binary image using the following:
If Bin(X, Y) = 1 Then tImg(X, Y) = 1 - tImg(X, Y)
I. Determine the Center Coordinates (X_{cen}, Y_{cen}) and Radius (R_d) for the iris pixels (i.e., the pixels whose binary value is 1):

```
Set Sx=0:  Sy=0:  n=0
For all X ϵ [0, ImgWid-1]
    For all Y ϵ [0, ImgHgt-1]
        If Bin(X, Y)=1  and  tImg(X, Y)=1  Then
            Sx=Sx+X:   Sy=Sy+Y:   n=n+1
        End if
    Next Y
Next X
```

$$X_{cen} = \frac{S_x}{n} \ , \quad Y_{cen} = \frac{S_y}{n} \ , \quad R_d = \sqrt{\frac{n}{\pi}}$$

J. Apply Radial Scan to Collect the External Boundary points, and then determine the radius array, Rad ().
K. Determine the mean (R_{mean}) and standard deviation (σ_{radius}) of all Radii collected within all sectors.
L. Re-determine the center coordinates (X_{cen}, Y_{cen}) and radius values (R_d), to get more Accurate Values. The following criterion has been applied to filter out the abnormal radii elements values and then re-determine the parameters (X_{cen}, Y_{cen}, R_d):

$$if\ |Rad(i) - R_{mean}| > 3\sigma_{radius}\ \ then\ \ exclude\ the\ i^{th}\ radius\ element$$

M. The determined center coordinates and radius are used as the geometric parameters for defining the external radius of the iris. They used to establish iris area mask which is circular area as shown in Figure-7.

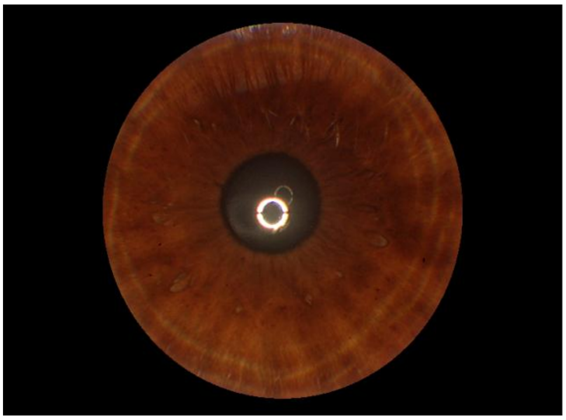

Figure 7- A Sample of Iris Isolated Area

4. Result and Discussion

A number of the iris images with different color and direction have been used In this study the standard dataset .The database contains 3 x 128 iris images (i.e.3 simple for the left iris and 3 sample for the right iris for (64) Persons).The images are: 24 bit - RGB, 576 x 768 pixels, file format: PNG. The irises were scanned by TOPCON TRC50IA optical device connected with SONY DXC-950P 3CCD camera [10]. Figure-8 illustrates the iris images (some data base images captured from left direction).

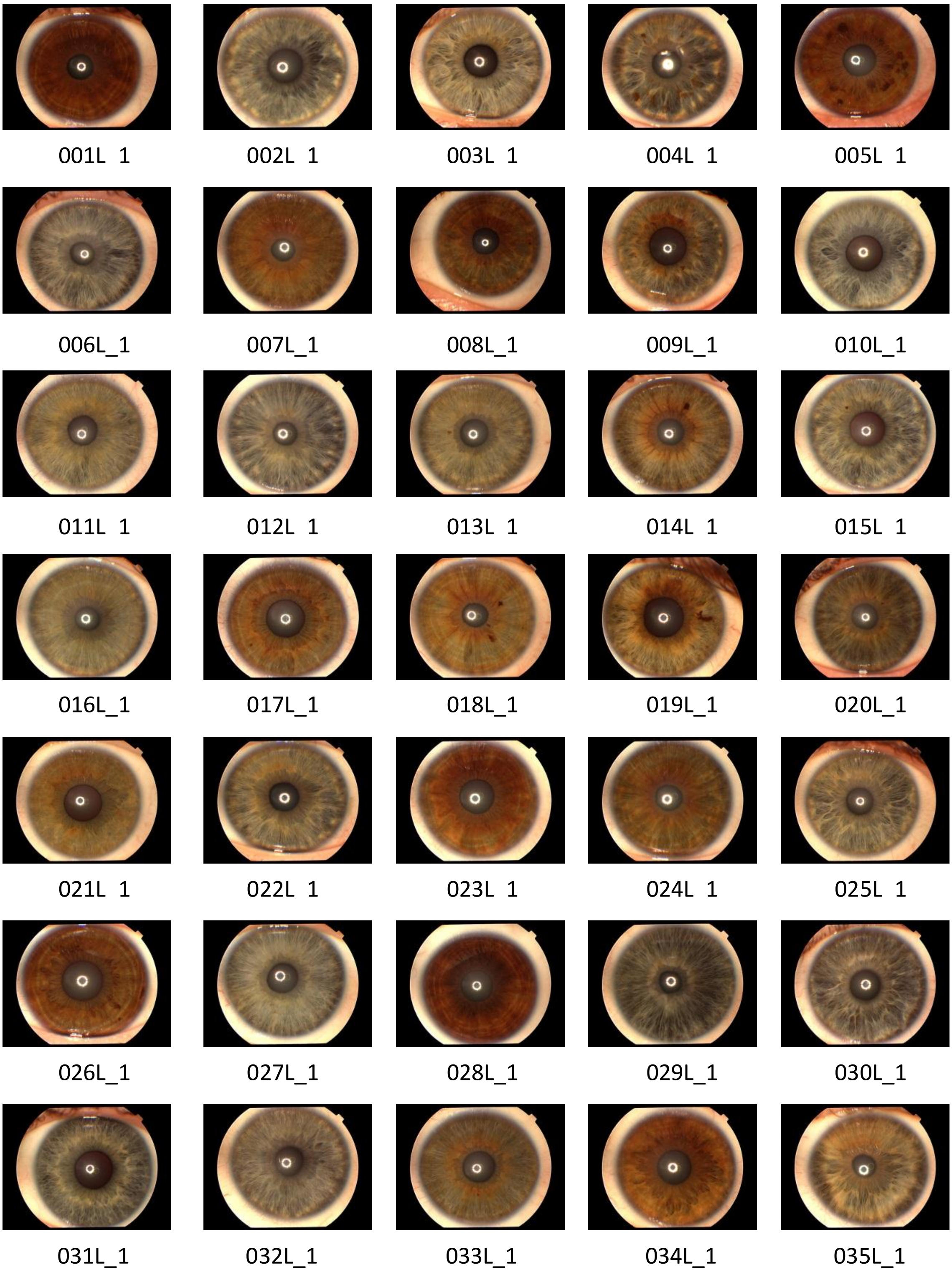

Figure 8- Some of the database images captured from left eye

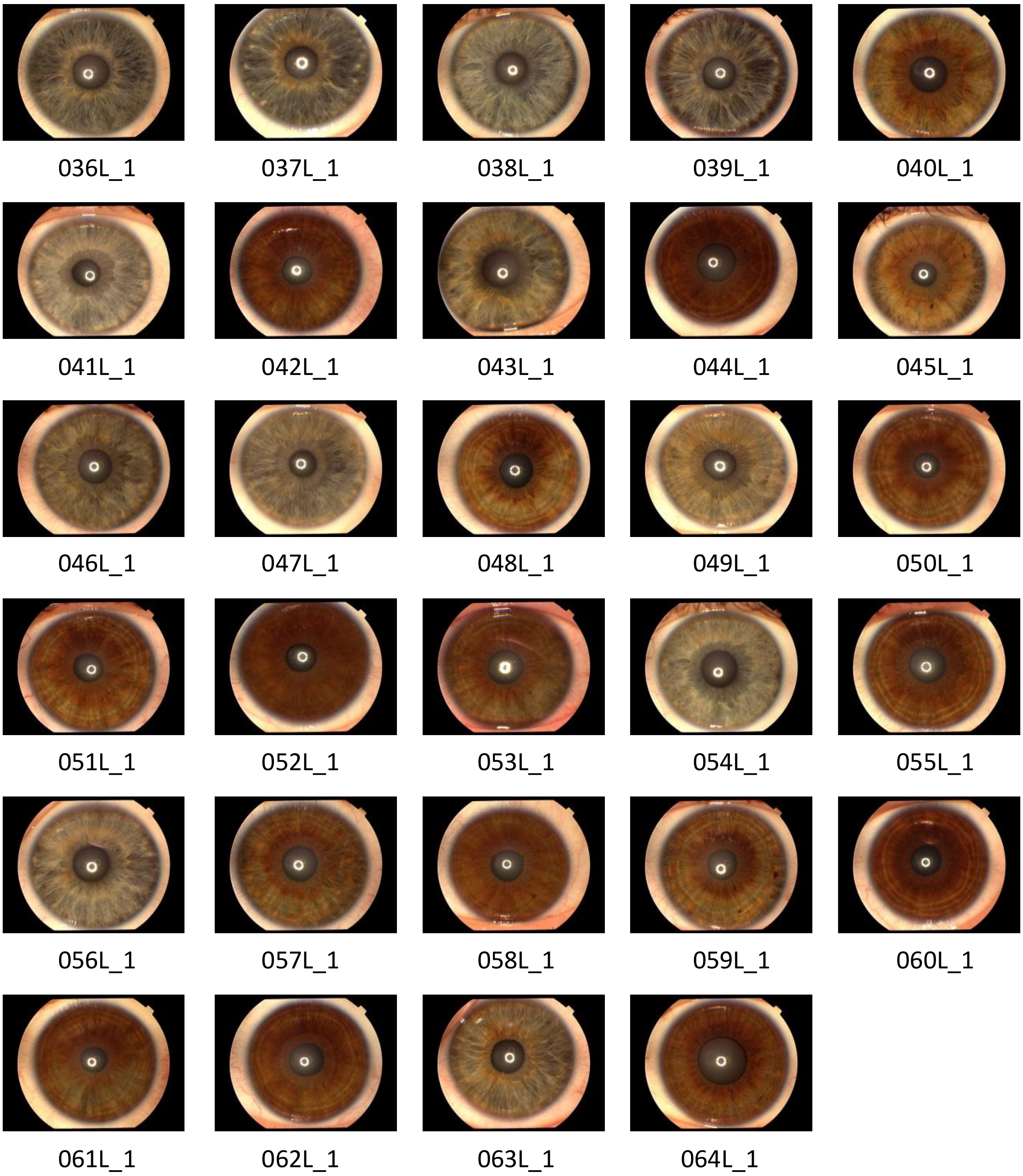

Figure 8- Some of the database images captured from left eye (continue)

Table-1 presents the mean (μ), standard division (σ) and the coefficient of variation (CV) for iris radius, from this table we can see the coefficient of variation (CV) values are small due to the high accuracy of the iris distinguish.

Table 1- The mean (μ), standard division (σ) and coefficient of variation (CV) for determined iris radius

No.	μ	σ	C.V	No.	μ	σ	C.V
1	245.366	4.063	0.0166	33	248.368	1.274	0.0051
2	243.913	1.316	0.0054	34	244.900	0.640	0.0026
3	244.601	7.140	0.0292	35	250.723	2.668	0.0106
4	249.300	2.848	0.0114	36	248.887	3.205	0.0129
5	246.774	3.062	0.0124	37	251.006	2.736	0.0109
6	244.507	2.887	0.0118	38	258.747	9.022	0.0349
7	254.618	1.246	0.0049	39	260.230	8.644	0.0332
8	238.187	4.879	0.0205	40	260.230	8.644	0.0142
9	238.669	3.778	0.0158	41	247.494	6.028	0.0244
10	246.709	3.147	0.0128	42	244.542	1.910	0.0078
11	246.826	2.226	0.0090	43	256.918	3.676	0.0143
12	250.206	1.543	0.0062	44	241.571	6.236	0.0258
13	251.216	5.188	0.0206	45	241.964	4.595	0.0190
14	253.342	3.458	0.0136	46	252.530	4.724	0.0187
15	250.129	1.341	0.0054	47	244.215	2.025	0.0083
16	250.615	6.202	0.0247	48	245.878	2.505	0.0102
17	249.464	1.931	0.0077	49	243.708	0.993	0.0041
18	246.205	3.627	0.0147	50	243.127	1.796	0.0074
19	246.936	17.125	0.0693	51	247.568	2.560	0.0103
20	249.239	8.309	0.0333	52	247.118	5.847	0.0237
21	239.916	4.128	0.0172	53	256.499	4.504	0.0176
22	252.797	1.151	0.0046	54	249.274	5.239	0.0210
23	245.984	1.211	0.0049	55	246.530	3.032	0.0123
24	250.573	1.257	0.0050	56	251.315	4.922	0.0196
25	238.714	9.779	0.0410	57	251.695	1.651	0.0066
26	249.314	2.452	0.0098	58	238.648	3.805	0.0159
27	253.718	1.576	0.0062	59	245.966	5.402	0.0220
28	243.645	4.908	0.0201	60	238.216	6.852	0.0288
29	246.618	3.864	0.0157	61	249.473	5.221	0.0209
30	241.315	4.190	0.0174	62	241.229	1.399	0.0058
31	253.175	7.484	0.0296	63	252.406	3.863	0.0153
32	248.888	1.775	0.0071	64	251.038	3.1469	0.0125

Figure-9 shows the histogram of the iris radii computed from the database images. The distribution is close to Gaussian (normal) distribution.

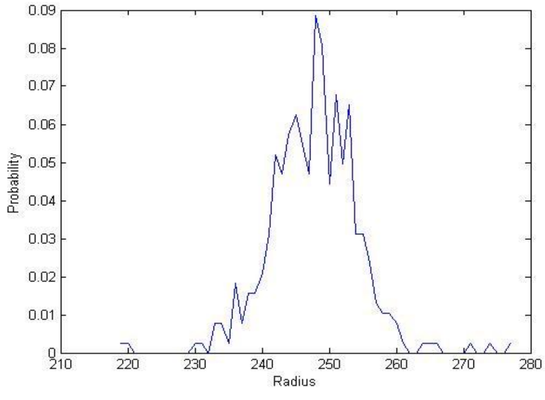

Figure 9- The histogram of the determined iris radius

5. Conclusion

In this study an efficient suggested method for iris detection for iris images. The results indicated the coefficient of variation (CV) normal distribution, and we can see the suggested algorithm has High accuracy in the iris detection.

References

1. Li Ma, Tieniu Tan, and Fellow. **2004**. Efficient Iris Recognition by Characterizing Key Local Variations. *IEEE Transactions on Image Processing*,13(6).
2. Jarjes, A.A., Kuanquan Wang , and Mohammed, G.J. **2010**.Iris localization: Detecting accurate pupil contour and localizing limbus boundary. *IEEE*, 1:349 - 352.
3. Davis-Silberman, N., and Ashery-Padan, R. **2008**. Iris Development Vertebrates Genetic and Molecular Considerations, *Brain Research*, 1192(5):1728.
4. Muron, A. and Pospisil, J. **2000**. The Human Iris Structure and Its Usages. 39:87-95.
5. Caroline, P. J. and André, M. P. **2002**. The Effect of Corneal Diameter on Soft Lens Fitting, Part1, *Contact Lens Spectrum*,17(4): 56.
6. Somying Thainimit, Luís A. Alexandre, and Vasco M. N. de Almeida. **2013**. Iris Surface Deformation and Normalization, *IEEE*, pp:501 – 506, 4-6.
7. Forrester J. V., Dick, A. D., McMenamin, P. G., and Lee, W. R. **2001**. *The Eye: Basic Sciences in Practice*, W.B. Saunders.
8. Maurice D., Weir, and Joel Hass. **2010**. *Thomas Calculus Early Transcendentals*, Twelfth Edition, Pearson Education.
9. Henrich, D.**1993**. Space-Efficient Region Filling in Raster Graphics. *The Visual Computer: An International Journal of Computer Graphics*.
10. Michal Dobeš and Libor Machala, Iris Database, website: *http://www.inf.upol.cz/iris/*.